Creep behaviour of single hemp fibres. Part I: Viscoelastic properties and their scattering under constant climate.

Ousseynou Cisse, Vincent Placet*, Violaine Guicheret-Retel, Frédérique Trivaudey, M. Lamine Boubakar

Department of Applied Mechanics, FEMTO-ST Institute, UMR CNRS 6174, University of Franche-Comté, F-25000 Besançon,

*Corresponding author: Email: vincent.placet@univ-fcomte.fr

tel: +33 (0)3 81 66 60 55 - fax: +33 (0)3 81 66 67 00

Code de champ modifié

ABSTRACT

The literature on the time-dependent behaviour of single bast fibres such as flax and hemp is extremely poor. The aim of this extensive study is to characterise the long-term behaviour of elementary hemp fibres and to establish suitable constitutive laws.

Single hemp fibres are shown to exhibit both instantaneous strain and delayed, time-dependent strain when tensile loaded under constant climate. The creep behaviour appears to be a logarithmic function of time with a high strain rate during the primary creep and a lower and constant one during the secondary creep. A large scattering both in time-dependent properties and behaviour was observed on a batch of 25 single fibres. Three main creep behaviours were observed. Type II is truly linear as a function of the logarithm of time while Type I and Type III are strongly nonlinear and can be described respectively by concave and convex functions. A rheological model based on an anisotropic viscoelastic law and on a truncated inverse Gaussian spectrum of viscous mechanisms was shown to successfully describe all the experimentally observed behaviours.

Key words: hemp fibres / creep / viscoelastic model

INTRODUCTION

Natural fibres derived from annual plants are attractive candidates to reinforce organic matrix in high performance composite applications. This use requires an accurate understanding of their mechanical properties and the development of efficient models. In the last years, many

efforts were concentrated on the characterisation of the tensile properties of bast fibres under quasi-static loading (*1-6*). In contrast, the time-dependent behaviour has almost not been examined (*7*). However, considering the polymeric composition of the fibre wall, it is probable that the fibres have significant viscoelastic behaviour. Plant fibres, like all polymeric materials, exhibit to greater or lesser extent viscoelastic behaviour. This point is of great importance in view of their integration in composite materials (*8-11*). Contrary to glass or carbon fibres reinforced plastics, the time-dependent behaviour of natural fibres reinforced plastics could arise both from the matrix and the fibres. So, the integration of the viscoelastic behaviour of natural fibres in the predictive mechanical models of natural fibre and natural fibres reinforced plastics is definitely necessary to ensure the reliability of the designed structures, in particular for long-term applications.

To the best of the authors' knowledge, only few results have been collected on the creep behaviour of plant fibre composites (*12-16*) and no information on the creep behaviour of cellulosic fibres derived from annual plants, such as hemp and flax, are available in literature. A few results were found on bamboo fibres (*17*). Yu et al. (*17*) showed the time dependency on the creep deformation of such fibres. They also emphasize the effect of moisture content on the creep behaviour. As sometimes hypothesized in literature, and considering some similarities in their organization and composition, the creep behaviour of bast fibres could also be similar to some of the wood fibres. However, this hypothesis needs to be confirmed. Anyway, the knowledge developed in the "wood" community can still be of great benefit to the "plant fibre reinforced polymers" community and a detailed state-of-the-art is required before starting any investigations on plant fibres. If the time-dependent behaviour of wood, wood tissue and paper has been widely studied from several decades (*18-21*), only a limited number of papers is related to the creep behaviour of single wood fibres (*22-27*). Their creep behaviour has been studied in the context of their use in the paper and packaging applications. Elementary wood fibre has been shown to exhibit both instantaneous elastic deformation and delayed, time-dependent deformation when subjected to an externally applied load, and a permanent strain when the load is removed (*22-24*). Wood fibres also exhibit increase in creep compliance with increasing moisture content. Several authors also observed much greater creep in cyclic humidity conditions than in a constant environment at the high-humidity extreme (*25-27*). This accelerated creep phenomenon, induced by the sorption and desorption of water in the fibre wall, is known as mechanosorptive (MCS) effect. So the time-dependent behaviour of wood fibres not only depends on the temperature, the loading history, the

moisture content but also on moisture content history as well as moisture variations. These parameters can interact and produce coupling effects (*18*).

So, the aim of this study is to investigate the time-stress-moisture dependent creep behaviour of elementary hemp fibres. The first part of this extensive study (Part I) proposes an experimental approach, using creep test under constant climate and stress. The aim of this first part is to provide the basis for the development of a constitutive law integrating the time-dependent behaviour of the single bast fibres derived from hemp plants. The second part of the study will be focused on the behaviour under variable climate and loading conditions.

MATERIALS AND METHODS

Plant material

Hemp fibres (Cannabis sativa L.) tested in this paper, were procured from the LCDA Company in France. They were delivered in a jumbled state. Bundles of fibres were washed in water for 72 h at 30°C in order to facilitate the extraction of elementary fibres. Single fibres were manually extracted and glued on thin paper supports.

Microscopic examination

The isolated single fibres were firstly examined using polarised light microscopy (Nikon Eclipse LV 150), to determine their outer diameters. The average diameter of each fibre was computed by taking ten measurements along its length.

Tensile creep test on elementary fibre

The time dependent characteristics can be measured by static tests or by Dynamic Mechanical Analysis (DMA). The behaviour of elementary hemp fibres has been widely studied in previous studies (*3*, *4*, *28*). Results showed a strong coupling between cyclic loading and moisture sorption. On this basis and also taking into account that the dynamic tests give a complex function in terms of frequency and that the conversion of dynamic results and conclusion to static, i.e. on a time scale, is not always obvious, we choose in this work to realise static tests.

A Dynamic Mechanical Analyser (DMA Bose Electroforce 3230) was used to perform the tensile creep/recovery and relaxation/blotting-out tests. In most of the experiments, creep/recovery tests were preferred to relaxation/blotting-out tests considering the problem of fibre buckling that can be encountered during blotting-out tests. No rotation of the fibre is

allowed during tensile loading. The paper frame supporting each elementary fibre was clamped onto the testing machine. Thereafter the fibre was conditioned to the required relative humidity up to the fibre reached moisture equilibrium. The time to reach the equilibrium was determined using isotherms of vapour water desorption/sorption. These tests are widely described in the second part of this work (Part II). The equilibrium was considered to be reached when the difference in mass between two measurements was less than 1%. The paper frame was cut before the beginning of each test. Several experiments were performed on carbon fibres to ensure that the glue and the extremity of the paper frame do not contribute to any creep.

The clamping length was 10 mm. The applied force was measured with a load sensor of 2 N with a resolution of about 1 mN, and the displacement was measured using a LVDT with a resolution of about 0.5 µm. To achieve the control of the environment around the natural fibres the machine was implemented with a relative humidity (RH) generator. The RH Generator (HumiSys HF from Instruquest Inc.) is designed to inject humidity inside the sample chamber using a heated transfer line with a flow rate between 500 ml/min and 5 l/min. The RH is controlled inside the sample chamber using a temperature and a humidity sensors placed inside the chamber, a few centimetres from the sample. The typical operating range is 10% to 90% (Fig. 1).

Fibres were subjected to static load. The sample elongation was measured and the strain calculated as the elongation divided by the initial fibre length. Tests were performed on fibres with an average external diameter of approximately 30 µm. The effective cross-section was determined using this mean external diameter assuming the fibre to be perfectly cylindrical and neglecting the lumen area. A fibre Area Correction Factor has recently been proposed for several plant fibres, such as for jute fibres, and shown to improve the prediction of the static properties of bast fibre composites (*29*). Such correction will be made when the factor will be determined for hemp fibres.

The stress was calculated using the applied force and the evaluated initial cross-section mean value of the fibre. Inside a same set of experiments, the applied load was calculated using the fibre cross-section to ensure a same stress for all the fibres. The loading rate used for each fibre corresponds to a stress rate of 50 $MPa.s^{-1}$. The duration of the dwell at this load level varied from 3 000 s to 40 000 s according to the tests. The variation of the cross-section during creep test was neglected.

VISCOELASTIC PROPERTIES IDENTIFICATION

Viscoelastic model

The deformation behaviour of linear viscoelastic materials is completely described by its creep function or its relaxation function. In this paper only the creep behaviour is considered. The creep function can be obtained using an appropriate model. In the literature, many models have been proposed to predict creep or relaxation functions of viscoelastic homogeneous and isotropic materials. For linear viscoelastic behaviour, these models can be divided into two main groups, (i) analytical expressions and (ii) rheological models made of series and parallel combinations of elastic springs and viscous dashpots or of springs and parabolic elements based respectively on exponential and power laws. For both, the unknown coefficients are determined through creep curves using curve-fitting techniques.

The rheological models which are the most commonly used for a one-dimensional medium and for the long-term viscoelastic behaviour are the generalized Kelvin-Voigt and Maxwell models and the multiparabolic model (*18*, *30*). In a parabolic model, it can be demonstrated that a generalised Maxwell model with a finite number of simple Maxwell elements is practically equivalent to a parabolic element. For these generalised rheological models and to keep a physical meaning, we generally consider that the rigidities respect a defined distribution as a function of the logarithm of time relaxation.

For materials such as the wall of hemp fibres, the use of an anisotropic constitutive law is more relevant. We propose to use the model developed by Boubakar et al. (*31*) and already applied to hemp fibres (*32*). Assuming that the local state of the material is completely defined by the elastic strain tensor $\underline{\varepsilon}^e$ and a set of second order tensors $\underline{\xi}_i$ ($i \in \mathbb{N}$) corresponding to N elementary mechanisms of viscoelastic flow, the state law leads to the following instantaneous constitutive equation :

$$\dot{\underline{\mathcal{E}}} - \dot{\underline{\mathcal{E}}}^{ve}(\underline{\xi}_i\,;\,\underline{\sigma}) = \underline{\underline{S}}\dot{\underline{\sigma}}, \tag{1}$$

where $\underline{\sigma}$ is the Cauchy true stress tensor, $\underline{\underline{S}}$ the elastic compliance tensor corresponding to a transverse isotropic behaviour with respect to the cellulose microfibrils direction, $\underline{\varepsilon}^{ve}$ the viscoelastic strain tensor and $\underline{\varepsilon}$ the total strain tensor such as $\underline{\varepsilon} = \underline{\varepsilon}^e + \underline{\varepsilon}^{ve}$.

Following (*31*), the viscoelastic flow rule is given by:

$$\dot{\underline{\varepsilon}}^{ve} = \sum_{i=1}^{N} \dot{\underline{\xi}}_i = \sum_{i=1}^{N} \frac{1}{\tau_i}\left(\mu_i \underline{\underline{S}}^{ve}\underline{\sigma} - \underline{\xi}_i\right), \tag{2}$$

where $\underline{\underline{S}}^{ve}$ is a viscoelastic compliance tensor whom general form is derived by considering an isotropic transverse behaviour with respect to the microfibrils direction, which is assumed to be purely elastic:

$$\underline{\underline{S}}^{ve} = \begin{pmatrix} 0 & 0 & 0 & 0 & 0 & 0 \\ 0 & \frac{\beta_T}{E_T} & -\frac{\beta_{TT}\nu_{TT}}{E_T} & 0 & 0 & 0 \\ 0 & -\frac{\beta_{TT}\nu_{TT}}{E_T} & \frac{\beta_T}{E_T} & 0 & 0 & 0 \\ 0 & 0 & 0 & \frac{\beta_{LT}}{G_T} & 0 & 0 \\ 0 & 0 & 0 & 0 & \frac{\beta_{LT}}{G_T} & 0 \\ 0 & 0 & 0 & 0 & 0 & \frac{\beta^*}{G_{TT}} \end{pmatrix}; \frac{\beta^*}{G_{TT}} = 2\left(\frac{\beta_T}{E_T} + \frac{\beta_{TT}\nu_{TT}}{E_T}\right) \quad (3)$$

Such a tensor requires, in addition to the classical elastic parameters, the identification of three new parameters ($\beta_T,\ \beta_{TT},\ \beta_{LT}$) related to the viscoelastic behaviour.

As given in equation 2, the effect of each elementary viscous mechanisms (i) is differentiated using weighting coefficients μ_i. The coefficients μ_i and the corresponding release time τ_i are obtained from different types of relaxation times spectrum layout. The spectral models tested and used in this work are: triangular (T), Gaussian (G), double-Gaussian (DG), inverse Gaussian (IG) distributions (Fig.2). The given μ_i are expressed with respect to $log(\tau_i)$ for spectrum T and $ln(\tau_i)$ for spectrums G, DG and IG.

For each case, the weighting functions are normalized by the following relation:

$$\sum_{i=1}^{N} \mu_i = 1 \quad (4)$$

where *N* represents the number of mechanisms of the viscoelastic model. In this study, *N* is not considered as a parameter and is fixed to 31. This value was empirically fixed to ensure enough accuracy.

The triangular spectrum is described by the centre n_c and the half-width n_0 of the triangle (*31*). The Gaussian and the inverse Gaussian spectrums are described by the mean τ_1 and the standard-deviation σ_d. Hence, μ_i are given by equation (5) for spectrum G and equation (6) for spectrum IG.

$$\mu_i = \frac{exp\left(-\frac{1}{2\sigma_d{}^2}(ln\tau_i - ln\tau_1)^2\right)}{\sum_{i=1}^{N} exp\left(-\frac{1}{2\sigma_d{}^2}(ln\tau_i - ln\tau_1)^2\right)} \quad (5)$$

$$\mu_i = \frac{exp\left(\frac{1}{2\sigma_d{}^2}(ln\tau_i - ln\tau_1)^2\right)}{\sum_{i=1}^{N} exp\left(\frac{1}{2\sigma_d{}^2}(ln\tau_i - ln\tau_1)^2\right)} \quad (6)$$

The double-Gaussian spectrum is the superposition of two Gaussian spectrum, described respectively by means values τ_1 and τ_2, and standard-deviation values σ_{d_1} andσ_{d_2}.

To complete the model, for each spectrum, two parameters are added in order to truncate the distributions differently at left and right sides. These parameters n_{min} and n_{max} are used to define the τ_{min} and τ_{max} boundaries of the distribution, as shown on figure 2 for both double-Gaussian and Inverse Gaussian spectrum. For the truncation, a half-width equal to $3\sigma_d$ for Gaussian type spectrum, corresponding to a trust level of around 99%, and the half-width n_0 for triangular spectrum are chosen. τ_{min} and τ_{max} boundaries are hence defined as

$log(\tau_{min}) = n_c - n_0 n_{min}$ and $log(\tau_{max}) = n_c + n_0 n_{max}$ for T spectrum

$ln(\tau_{min}) = ln(\tau_1) - 3\sigma n_{min}$ and $ln(\tau_{max}) = ln(\tau_1) + 3\sigma n_{max}$ for G and IG spectrums

$ln(\tau_{min}) = ln(\tau_1) - 3\sigma_1 n_{min}$ and $ln(\tau_{max}) = ln(\tau_2) + 3\sigma_2 n_{max}$ for DG spectrum

Both n_{min} and n_{max} are real number comprised between 0 and 1. The N mechanisms are equally distributed between these two boundaries. The parameters describing the spectrum for each case are summarized in Table 1.

Creep function-fitting procedure

Two scalar independent creep functions have to be experimentally determined to characterize anisotropic time-dependent behaviour of hemp fibres. Laborious experimentations work has to be performed to determine these functions, in particular to determine the transverse creep function. In this study, we are only working with the experimentally determined axial creep function. The theoretical axial viscoelastic compliance $J_{ZZ}(t)$ is expressed as follows:

$$J_{ZZ}(t) = \frac{\varepsilon_{ZZ}^{ve}(t)}{\sigma_0} = \frac{\sum_{i=1}^{31} \mu_i S_{ZZ}(1 - e^{-\frac{t}{\tau_i}})}{\sigma_0} \quad (7)$$

where $S_{zz} = \frac{\beta_T}{E_T}\cos^4(\psi) + \frac{\beta_{LT}}{G_{LT}}\cos^2(\psi)\sin^2(\psi)$ (8)

ψ is the supplementary angle of the cellulose Microfibrils Angle (MFA) and σ_0 the constant axial stress.

On the basis of the axial viscoelastic compliance, only S_{zz} parameter can be identified (Eq. 8). This parameter was identified using the aforementioned model and a hybrid optimisation algorithm. In order to avoid convergence towards local optima in the case of multimodal test functions, the Levenberg-Marquardt algorithm was combined with a heuristic method based on a genetic algorithm (Fig. 3). This hybrid algorithm is described in (*33*, *34*), and involves minimisation of the objective function *f* (Eq. 9).

$$f = \frac{\sqrt{\sum_{k=1}^{n}\left(\frac{J_{ZZ_{exp}}^{k} - J_{ZZ_{mod}}^{k}}{\max(J_{ZZ_{exp}}^{k})}\right)^2}}{2n} \quad (9)$$

where $J_{ZZ_{exp}}^{k}$ is the kth value of the experimental compliance data, $J_{ZZ_{mod}}^{k}$ is the kth computed value using the aforementioned model, and *n* is the number of elements in the dataset.

To perform the identification of the parameters, the inverse identification strategy for restricted or redundant data proposed in (*35*) is used. The parameters to be identified are the spectrum parameters, as described previously and the material parameter S_{ZZ} (Table 1).

RESULTS AND DISCUSSION

Creep / recovery

Fig. 4 shows the evolution of the fibre strain when submitted to a typical creep-recovery test. During the recovery step, a small tensile load is maintained to avoid buckling of the fibre. When loaded, the fibre exhibits both instantaneous strain and delayed, time-dependent strain. With stress, sufficient energy is supplied to overcome secondary bonds which define the

initial macromolecular structure of the amorphous components. The packing molecules tend to align themselves in the direction of the stress by moving into new positions. The extension is found to increase rapidly at first (during the 15 first minutes) and more slowly after. These two creep components are classically called primary creep and secondary creep. For reason of time, the tertiary creep is not considered in this study. As in many cases (*22, 23, 27*), the creep of elementary hemp fibres appears as a logarithmic function of time. When the load is removed, the fibre contracts, more quickly at first (during the first minutes) again. However the retraction rate after the first time of recovery is higher than for the secondary creep.

Our results also clearly show that, even after a prolonged time of retraction, a significant residual extension or permanent set remains. The instantaneous recovery, when the applied load is released, is extremely small in comparison to the initial instantaneous strain. Only a portion of the delayed strain is recovered after 3 hours. The existence of irreversible strain was already observed for these fibres under monotonic tensile loading (*36*). This was attributed to complex phenomena involving stick-slip mechanisms (*37*) and strain-induced crystallisation of cellulose. In the amorphous regions, and after the molecular reorganisation induced by stress, the bond reformation is assumed to be associated to a lock-in phenomenon. This could explain the large permanent set observed upon removal of the external stress.

For most of the viscoelastic materials, the primary creep is considered as the time-dependent recoverable portion of the delayed strain, as the secondary creep is the portion of the total sample strain which is non-recoverable at the test conditions after removal of the load. For hemp fibre, as a consequence of the lock-in phenomenon, a portion of the primary creep is also non recoverable.

Whatever its physical or microstructural origin, these time-dependent phenomena with large permanent set could affect the dimensional stability and other performance characteristics of natural fibres reinforced composites, and has to be taken into account.

Scattering in creep response

Fig.5 shows the creep response of 25 elementary fibres when submitted to a constant load (corresponding to an initial tensile stress of 50 MPa). Fig.5a. plots the evolution of the viscoelastic compliance as a function of time, Fig.5b. the normalized compliance as function of time and Fig.5c. as a function of the logarithm of time. Tab. 2 synthesises the creep properties determined from these curves, i.e. the instantaneous apparent Young's modulus, the

total, instantaneous and time-delayed strains. A high scattering both in creep behaviour and in creep properties is observed.

Based on the mean values, and for the considered creep time (3600 s), the time-delayed strain is of the same order in magnitude than the instantaneous one (0.48% vs. 0.53%). The coefficient of variation is slightly higher for the time-delayed strain and reaches a value of approximately 80%. This dispersion can partially be induced by the experimental technique used for the strain determination (elongation measured from the crosshead displacement). It can also be due to variation in the cell wall geometry and composition along the fibre length which could cause stress and strain heterogeneities.

Fig. 5b and 5c also point out the large difference in the primary and secondary creep rates. The decrease in the primary creep rate as a function of time varies also strongly from one fibre to another. It traduces large differences in relaxation times. Using a logarithmic timeline, it clearly appears that three different creep behaviours can be observed. Type II is truly linear as a function of the logarithm of time.Type I and Type III are strongly nonlinear. Type I is described by a concave function and Type III by a convex one. Three types of monotonic tensile behaviour were already observed for hemp fibres (*36, 38-40*). The origin of these different behaviours is unknown. The hypothesis of maturity, or the position of the fibres in the stem, could be considered. Indeed, technical fibres are composed of primary and secondary fibres, both originating from the phloem. These two different types of bast fibres (primary and secondary fibres) found in hemp have different and independent types of development, and also have different morphological and biochemical compositions which could lead to different mechanical behaviours (*41*). The different creep behaviours observed in this work could result from the same origins.

We propose in the next part of this paper to describe these typical behaviours using an anisotropic viscoelastic model.

Modelling

A few creep curves referred to the extreme time-delayed behaviours (Types I, II and III) and also with extreme amplitudes in strain were selected to identify a viscoelastic model able to fit and describe all the experimental curves. For each selected creep curve, the identification strategy is applied for the four types of spectrum presented previously, by launching the

hybrid algorithm ten times. For the discussion, the results corresponding to the minima of the objective function (residue) are retained.

The experimental creep curves and those obtained by the proposed modelling are compared (Fig. 6). In parallel, in order to compare the different spectrum, Table 3 gives the value of the residue obtained in each case. The results show that the triangular spectral model is inappropriate to fit all types of creep curves (Fig. 6). The Gaussian spectral model gives relatively good results but less satisfying than double-Gaussian and inverse Gaussian models. These latter give similar results. Inverse Gaussian model will be preferred rather than double-Gaussian which needs more parameters to be identified. Several authors, such as Bardet et al. (*30, 42*) for wooden materials, used a double spectral model in order to represent two viscoelastic mechanisms involved in the time-delayed response. These mechanisms are described by different release times. The inverse Gaussian spectral model that we proposed in this work is also able to balance two main release times but with a single spectral distribution, thereby limiting the number of shape parameters.

Figure 7 shows the mechanisms distributions for the inverse Gaussian spectral model, obtained for the three types of creep curves. As expected, the truncation influences the shape of the curve. The concavity of Type I is obtained by a truncation of the right branch of the spectrum, as the convexity of Type III is obtained by a truncation at the left side. Type II, which is linear is represented by a quasi-constant spectrum. The identified parameters (Tab. 4) confirm the large difference in viscoelastic compliance and relaxation times qualitatively noticed in the previous paragraph, when describing the experimental creep functions. The values of the identified axial component of the viscoelastic compliance (S_{ZZ}) and of the time constant τ_1 are respectively 1.6 10^{-4} MPa^{-1} and 563 s for Type I and 2.4 10^{-5} MPa^{-1} and 5.6 s for Type III. These results seem to reflect the existence of several viscoelastic mechanisms, with different time constants, which can express more or less as a function of the fibre under constant environmental conditions. The physical or macromolecular origin of these mechanisms remains to be defined. Anyway, the proposed model allows two mains release times to be balanced.

CONCLUSION

Single hemp fibres exhibit significant delayed strain when submitted to tensile load. When the fibres are unloaded, large permanent strains are observed. This unrecoverable strain originates

from instantaneous and time-dependent mechanisms since only a portion of both instantaneous and delayed strains is recovered

The creep behaviour appears to be a logarithmic function of time with a high strain rate during the primary creep and a lower and constant one during the secondary creep.

A large scattering both in time-delayed strains and behaviour was observed on a set of single fibres tested under constant climate. Three main creep behaviours were observed. Type II is truly linear as a function of the logarithm of time while Type I and Type III are strongly nonlinear and can be described respectively by a concave and a convex function. A rheological model based on anisotropic viscoelastic law and on a truncated inverse Gaussian spectrum of viscous mechanisms was shown to successfully describe all the experimentally observed behaviours.

The influence of stress level and climate conditions on the time-delayed behaviour will be characterized in the next part of this work.

ACKNOWLEDGEMENTS

The authors would like to thank Camille Garcin from the FEMTO-ST for his assistance with some of the experiments.

REFERENCES

1. Baley C (2002) Analysis of the flax fibres tensile behaviour and analysis of the tensile stiffness increase. Composites Part A: Applied Science and Manufacturing 33(7):939
2. Silva FdA, Chawla N, Filho RDdT (2008) Tensile behavior of high performance natural (sisal) fibers. Composites Science and Technology 68:3438
3. Placet V (2009) Characterization of the thermo-mechanical behaviour of Hemp fibres intended for the manufacturing of high performance composites. Composites Part A: Applied Science and Manufacturing 40(8):1111
4. Placet V, Cisse O, Boubakar ML (2012) Influence of environmental relative humidity on the tensile and rotational behaviour of hemp fibres. Journal of Materials Science 47(7):3435
5. Nilsson T, Gustafsson PJ (2007) Influence of dislocations and plasticity on the tensile behaviour of flax and hemp fibres. Composites Part A: Applied Science and Manufacturing 38(7):1722
6. Virk AS, Hall W, Summerscales J (2010) Failure strain as the key design criterion for fracture of natural fibre composites. Composites Science and Technology 70(6):995

7. Nilsson T (2006). Micromechanical modelling of natural fibres for composite materials. PhD thesis, Lund.

8. Shah D (2013) Developing plant fibre composites for structural applications by optimising composite parameters: a critical review. Journal of Materials Science 48(18): 6083

9. Summerscales J, Dissanayake NPJ, Virk AS, Hall W 2010) A review of bast fibres and their composites. Part 1- Fibres as reinforcements. Composites Part A: Applied Science and Manufacturing 41(10):1329

10. Summerscales J, Dissanayake N, Virk A, Hall W (2010) A review of bast fibres and their composites. Part 2 - Composites. Composites Part A: Applied Science and Manufacturing 41(10):1336

11. Summerscales J, Virk A, Hall W (2013) A review of bast fibres and their composites: Part 3- Modelling. Composites Part A: Applied Science and Manufacturing 44 (0):132

12. Gassan J, Bledzki AK (1999) Influence of fiber surface treatment on the creep behavior of jute fiber-reinforced polypropylene. Journal of Thermoplastic Composite Materials 12(5):388

13. Scott DW, Lai JS, Zureick AH (1995) Creep behavior of fiber-reinforced polymeric composites: a review of the technical literature. Journal of Reinforced Plastics and Composites 14(6):588

14. Takemura K (2004) Effect of water absorption on static and creep properties for jute fiber reinforced composite. WIT Transactions on the Built Environment / High Performance Structures and Materials II:7

15. Takemura K (2006) Effect of surface treatment to tensile static and creep properties for jute fiber reinforced composite. WIT Transactions on the Built Environment / High Performance Structures and Materials III: 7

16. Takemura K, Miyamoto S, Katogi H (2013) Effect of Surface Treatment on Creep Property of Jute Fiber Reinforced Green Composite under Environmental Temperature. Key Engineering Materials 525:53

17. Yu Y, Jiang Z, Fei B, Wang G, Wang H (2011) An improved microtensile technique for mechanical characterization of short plant fibers: a case study on bamboo fibers. Journal of Materials Science 46(3):739

18. Navi P, Stanzl-Tschegg S (2008) Micromechanics of creep and relaxation of wood. A review COST Action E35 2004–2008: Wood machining – micromechanics and fracture. Holzforschung 63(2):186

19. Holzer S, JR L, Dillard D 1989) A Review of creep in wood : concepts relevant to develop long-term behavior predictions for wood structures. Wood Fiber Sciences 21(4):376

20. Ansell M (2011). Wood - a 45th anniversary review of JMS papers. Part 1: The wood cell wall and mechanical properties. Journal of Materials Science 46(23):7357

21. Haslach H, Jr (2000) The Moisture and Rate-Dependent Mechanical Properties of Paper: A Review. Mechanics of Time-Dependent Materials 4(3):169

22. Sedlachek K, Ellis R (1994) The effect of cyclic humidity on the creep of single fibers of Southern pine. In: Fellers C LT, ed. Moisture-induced creep behaviour of paper and board. Stockholm: STFI, USDA, 1994:22.

23. Sedlachek K (1995) The effect of hemicelluloses and cyclic humidity on the creep of single fibres. Inst Paper Sci Technol: Georgia Tech.

24. Coffin D, Boese S (1997) Tensile creep behavior of single fibers and paper in a cyclic humidity environment. 3rd Int. Symp. On Moisture and Creep effects on paper and containers. Rotorua, New-Zealand.

25. Haberger C, Coffin D, Hojjatie B (2001) Influence of humidity cycling parameters on the moisture-accelerated creep of polymeric fibers. J Polym Sci Pol Phys 39:2048

26. Olsson A-M, Salmén L, Eder M, Burgert I (2007) Mechano-sorptive creep in wood fibres. Wood Science and Technology 41(1):59

27. Dong F, Olsson A-M, Salmén L (2010) Fibre morphological effects on mechano-sorptive creep. Wood Science and Technology 44(3):475

28. Placet V (2010) Tensile behaviour of natural fibres. Effect of loading rate, temperature and humidity on the "accommodation" phenomena. International Conference on Experimental Mechanics. Poitiers.

29. Virk A, Hall W, Summerscales J (2012) Modulus and strength prediction for natural fibre composites. Materials Science and Technology 28(7):864

30. Bardet S (2001) Comportement thermoviscoélastique transverse du bois humide. PhD thesis, Montpellier II, France.

31. Boubakar ML, Vang L, Trivaudey F, Perreux D (2003) A meso-macro finite element modelling of laminate structures: Part II: time-dependent behaviour. Composite Structures 60(3):275

32. Trivaudey F, Placet V, Guicheret-Retel V, Boubakar L (2014) Nonlinear tensile behaviour of elementary hemp fibres. Part II: Modelling using an anisotropic viscoelastic constitutive law in a material rotating frame. Composites Part A, In Press.

33. Carbillet S (2005) Contribution aux calculs fiabilistes sur des structures composites. PhD thesis, University Franche-Comté.

34. Richard F (1999) Identification du comportement et évaluation de la fiabilité des composites stratifiés. PhD thesis, University Franche-Comté.

35. Carbillet S, Guicheret-Retel V, Trivaudey F, Richard F, Boubakar L (2014) Identification of highly non-linear behavior models with restricted or redundant data. Information Sciences, In Press.

36. Placet V, Cisse O, Boubakar L (2014) Nonlinear tensile behaviour of elementary hemp fibres. Part I: Investigation of the possible origins using repeated progressive loading with in situ microscopic observations. Composites Part A: Applied Science and Manufacturing 56:319

37. Keckes J, Burgert I, Fruhmann K, et al (2003) Cell-wall recovery after irreversible deformation of wood. Nature Materials 2(12):810

38. Duval A, Bourmaud A, Augier L, Baley C (2011) Influence of the sampling area of the stem on the mechanical properties of hemp fibers. Materials Letters 65(4):797

39. Marrot L, Lefeuvre A, Pontoire B, Bourmaud A, Baley C (2013) Analysis of the hemp fiber mechanical properties and their scattering (Fedora 17). Industrial Crops and Products 51(0):317

40. Beckermann GW, Pickering KL (2008) Engineering and evaluation of hemp fibre reinforced polypropylene composites: Fibre treatment and matrix modification. Composites Part A: Applied Science and Manufacturing 39(6):979

41. Placet V, Méteau J, Froehly L, Salut R, Boubakar ML (2014) Investigation of the internal structure of hemp fibres using optical coherence tomography and Focused Ion Beam transverse cutting. Journal of Materials Science 49(24):8317

42. Bardet S, Gril J (2002) Modelling the transverse viscoelasticity of green wood using a combination of two parabolic elements. Comptes Rendus Mécanique 330(8):549

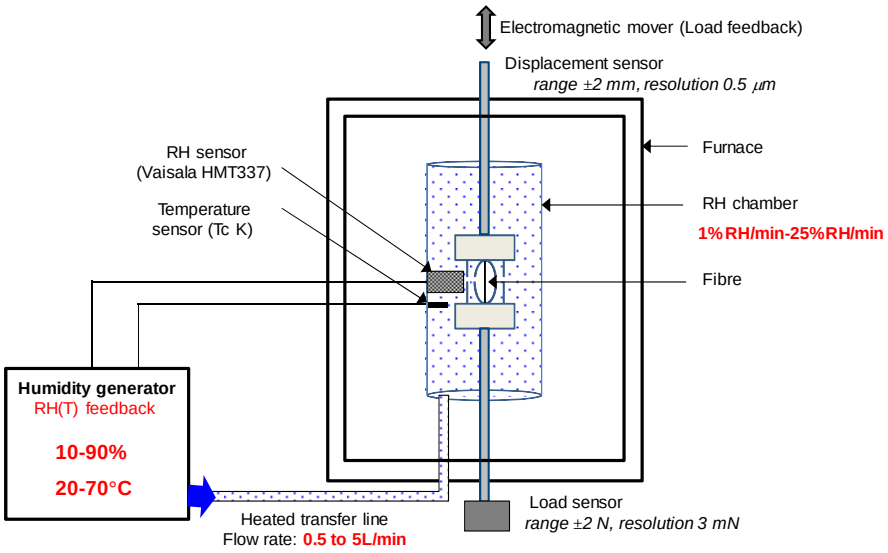

Figure 1: Schematic representation of the experimental set-up for the characterisation of the time-humidity dependent behaviour of single bast fibres

a.

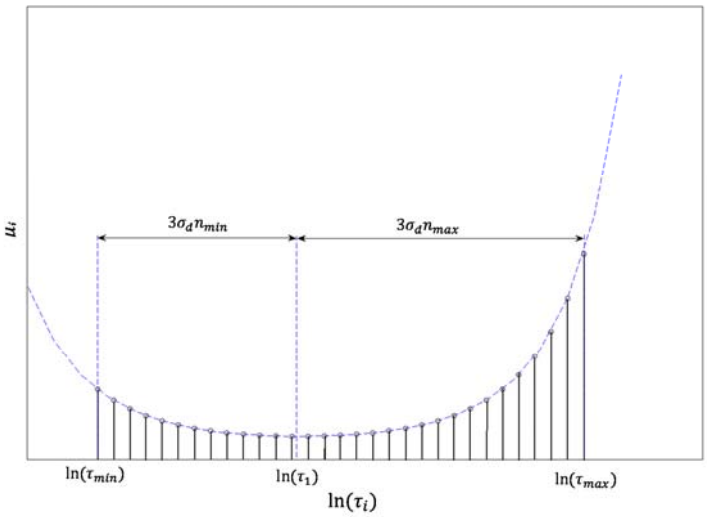

b.

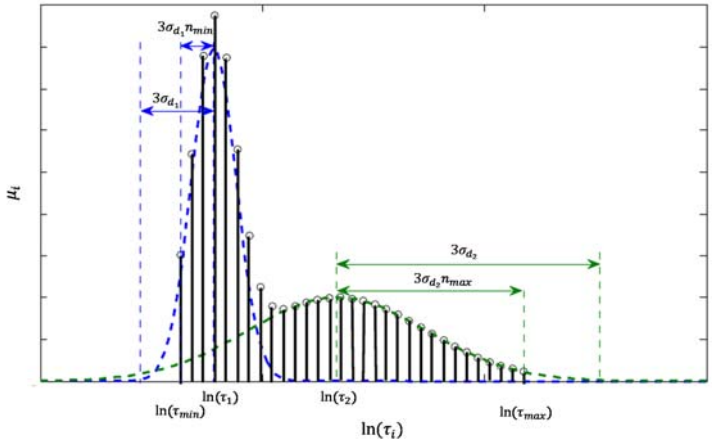

Figure 2 : Spectral models. a. Inverse Gaussian spectrum. b. Double-Gaussian spectrum.

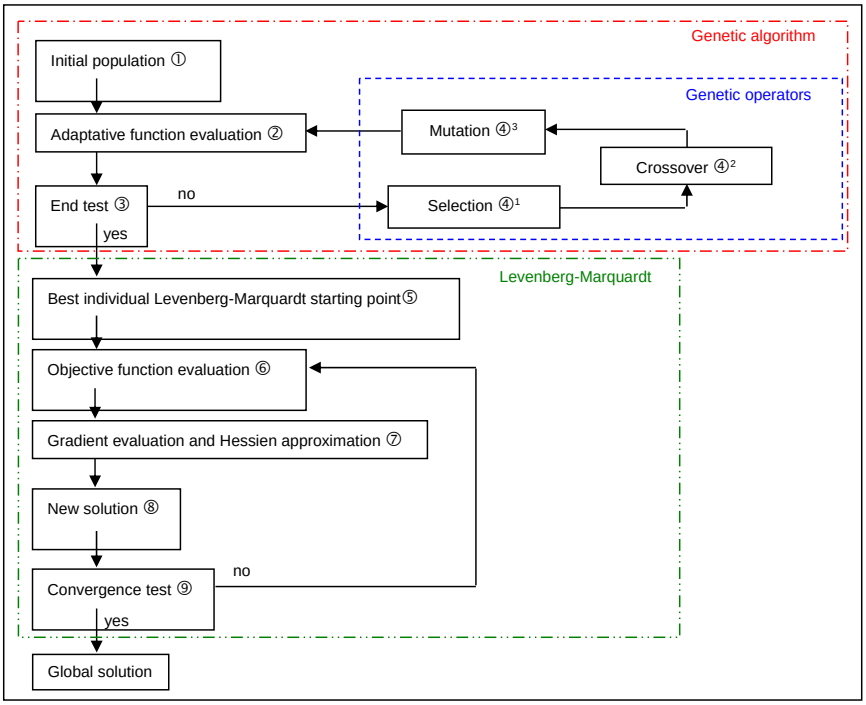

Figure 3: Identification procedure for the parameters of the spectral model

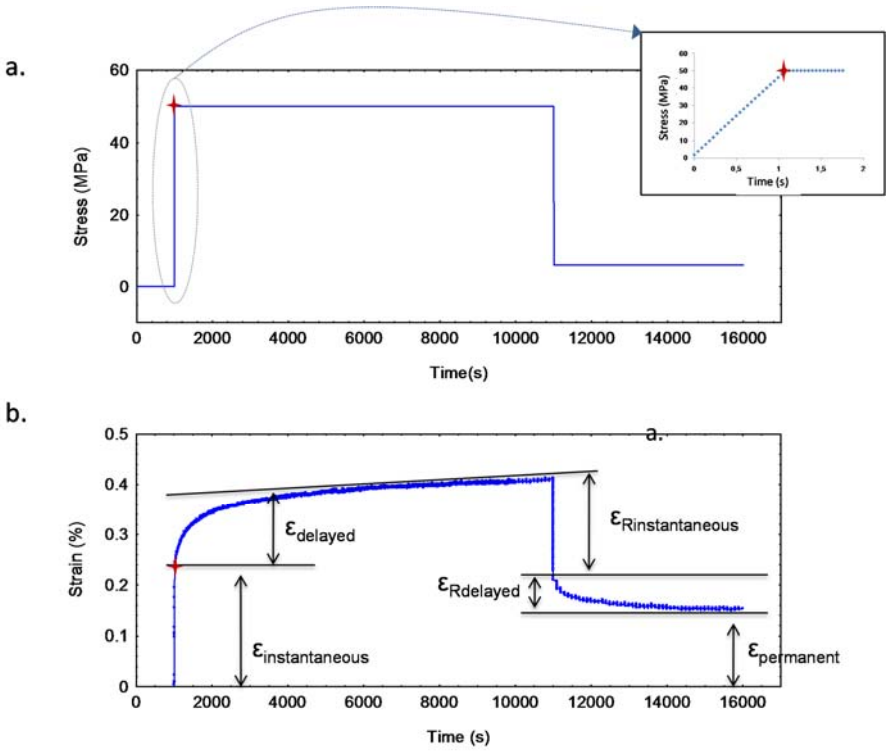

Figure 4: Creep-recovery test on a single hemp fibre. Evolution of tensile load (a) and strain (b) as a function of time (T=23°C ±1.5°C)

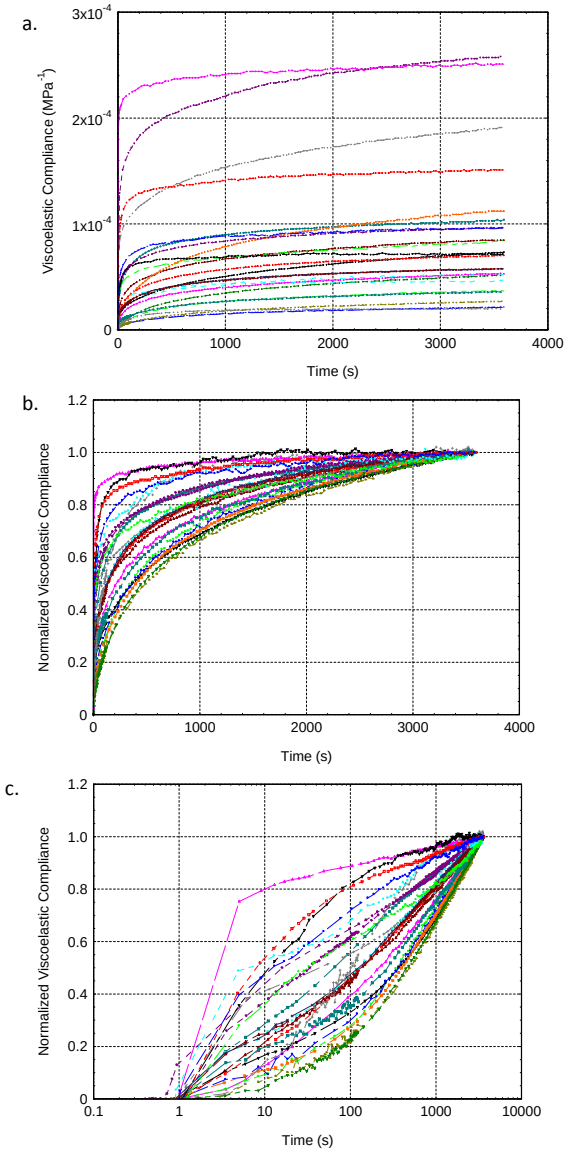

Figure 5: a. Evolution of the creep strain of 25 elementary hemp fibres as a function of time (Constant load corresponding to an initial tensile stress of 50 MPa, T=23°C ±1.5°C, RH=50% ±2.5%) showing a large scattering in response. b. Normalized viscoelastic compliance as a function of time. c. Normalized viscoelastic compliance as a function of the logarithm of time. Evidence of three types of response: linear (I), nonlinear convex (II), nonlinear concave.

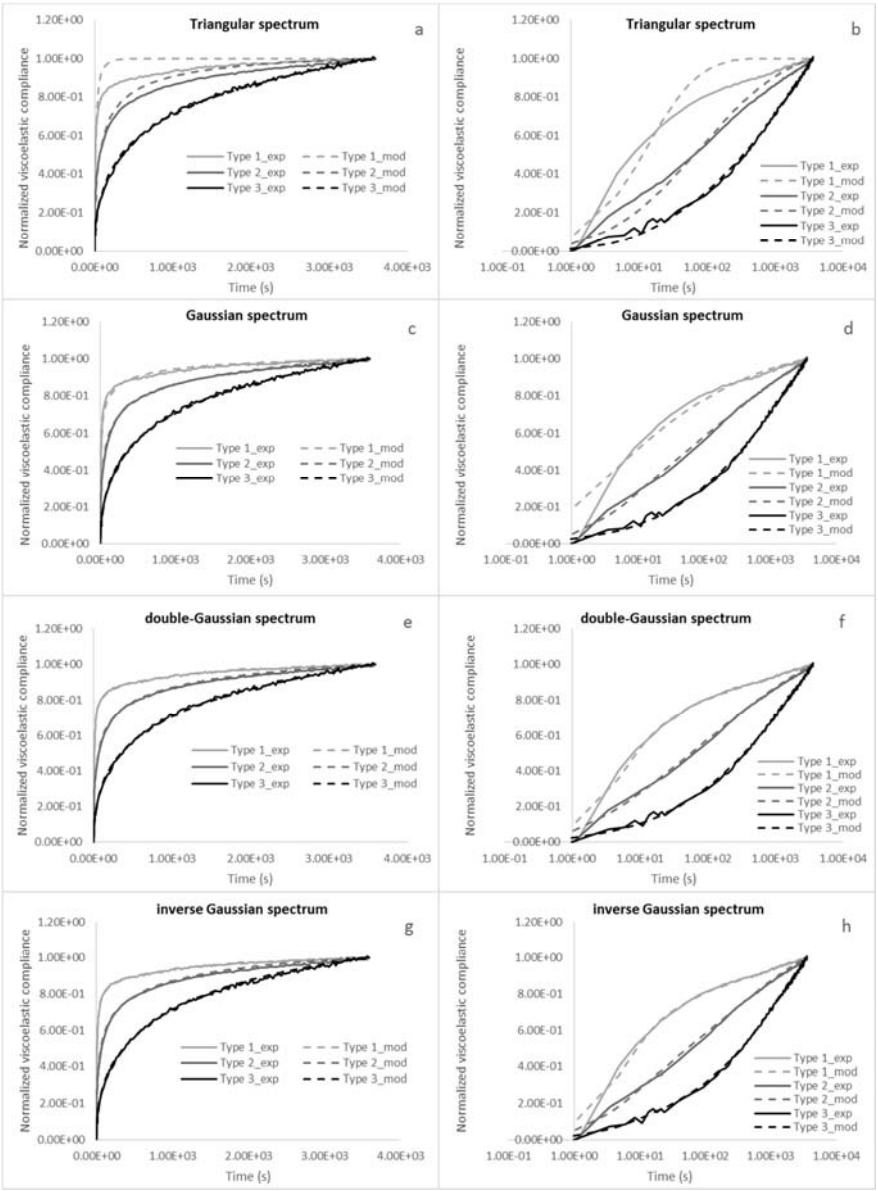

Figure 6: Comparison between experimental curves (types I, II and II) and the different spectral models (triangular, Gaussian, double-Gaussian, inverse-Gaussian)- a, c, e, g : Normalized viscoelastic compliance as a function of time. b, d, f, h : Normalized viscoelastic compliance as a function of time with a logarithm scale.

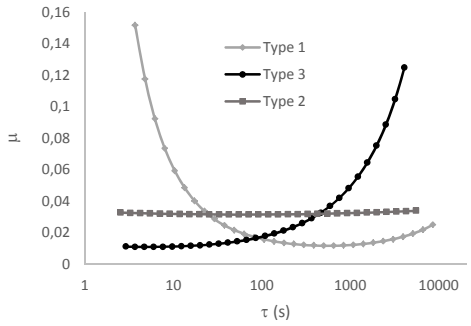

Figure 7: Inverse Gaussian distribution functions identified for each typical experimental curve

Table 1 : Parameters of the viscoelastic model and of the different spectrum.

	T spectrum	G spectrum	DG spectrum	IG spectrum
Spectrum parameters	n_c n_0	τ_1 σ_d	τ_1 τ_2 $\sigma_{d_1}\sigma_{d_2}$	τ_1 σ_d
Truncation parameters	n_{min} n_{max}			
Material parameters	S_{ZZ}			

Table 2 : Creep properties determined on a set of 25 elementary fibres submitted to a constant load (corresponding to an average tensile stress of 50 MPa)

	External diameter (μm)	Instantaneous apparent Young's modulus (GPa)	Total strain (%)	Instantaneous strain (%)	Time-delayed strain (%)
Mean value ±Standard Deviation *Min… Max*	**30** ±8.8 *14.8…44.7*	**16** ±8.4 *2.7…30*	**1.02** ±0.61 *0.23…2.3*	**0.53** ±0.36 *0.14…1.58*	**0.48** ±0.4 *0.2…1.34*

Table 3 : Curve-fitting residue for the 3 typical experimental curves and for the spectral models (triangular, Gaussian, double-Gaussian, inverse Gaussian).

Creep curve-type	triangular	Gaussian	double-Gaussian	inverse Gaussian
1	$1.3\ 10^{-5}$	$3.4\ 10^{-6}$	$9.1\ 10^{-7}$	$9.5\ 10^{-7}$
2	10^{-6}	$6.4\ 10^{-7}$	$6.4\ 10^{-7}$	$5.7\ 10^{-7}$
3	$3.5\ 10^{-6}$	$4.7\ 10^{-7}$	$3.6\ 10^{-7}$	$4.2\ 10^{-7}$

Table 4 : Fitted parameters for the different creep curve-types for inverse Gaussian spectral model

Creep curve-type	τ_1 (s)	σ_d (s)	n_{min}	n_{max}	S_{ZZ} (MPa^{-1})
1	562.9	2.2	0.79	0.37	$1.6\ 10^{-4}$
2	64.3	11.6	0.10	0.12	$1.1\ 10^{-4}$
3	5.6	3	0.10	0.71	$2.4\ 10^{-5}$